Low temperature methane oxidation on differently supported 2 nm Au nanoparticles

G. Walther[1], L. Cervera-Gontard[2], U.J. Quaade[3], S. Horch[1,3,*]

[1] Center for Atomic-scale Materials Design (CAMD), Department of Physics
[2] Center for Electron Nanoscopy (CEN)
[3] Center for Individual Nanoparticle Functionality (CINF), Department of Physics
Technical University of Denmark, DK-2800 Kgs. Lyngby, Denmark

* Corresponding author: horch@fysik.dtu.dk

Abstract

Low temperature CH_4 oxidation was studied on 2 nm gold nanoparticles supported on various metal-oxides. The differences in reaction rates for the different systems suggest that the support material has an effect on the activity. From TEM analysis, we found that the gold particles were stable in size during the reaction. In addition to full oxidation to CO_2, traces of C_2H_6 were detected when Au/TiO_2 was used, indicating limited partial CH_4 oxidation. TiO_2 was found to be the best support for gold nanoparticles both in terms of activity and gold particle stability.

Keywords: Gold; TiO_2; Al_2O_3; ZnO; Catalysis; Methane; Oxidation; Particle size

Introduction

All fossil fuels are mixtures of hydrocarbons. CH_4 is the most difficult of all hydrocarbons to oxidize. It is obvious that CH_4 is a much more suitable fuel source concerning its higher atomic ratio of H:C. Natural gas sources that mainly consist of CH_4, are so remote from the consumers that transportation of LNG (liquefied natural gas) is often uneconomic. Natural gas that is produced along with oil, is often flared and accounts with more than 20 billion cubic meters annually, and this has a significant detrimental effect on the environment [1]. Thus, there is a keen interest in converting CH_4 catalytically into higher valuable chemicals [2, 3], e.g. methanol, that is one of the seven building blocks in organic chemistry [4]. The reason why no good catalyst has been developed for low temperature partial CH_4 oxidation as yet is the higher reactivity of the products (CH_3OH and HCHO) compared to CH_4 [5]. Thermodynamically, complete combustion to CO_2 and H_2O is more favorable:

$$CH_4 + {}^1/_2\, O_2 \rightarrow CH_3OH \qquad \Delta H^0 = -126.4 \text{ kJ mol}^{-1} \quad (1)$$
$$CH_4 + O_2 \rightarrow HCHO + H_2O \qquad \Delta H^0 = -284.2 \text{ kJ mol}^{-1} \quad (2)$$
$$CH_4 + {}^3/_2\, O_2 \rightarrow CO + 2\, H_2O \qquad \Delta H^0 = -519.3 \text{ kJ mol}^{-1} \quad (3)$$
$$CH_4 + 2\, O_2 \rightarrow CO_2 + 2\, H_2O \qquad \Delta H^0 = -802.3 \text{ kJ mol}^{-1} \quad (4)$$

There are not very many studies dealing with CH_4 oxidation on gold, although gold has been shown to be surprisingly active for many other reactions, especially CO oxidation [6–24] and oxidation of hydrocarbons [8, 16, 17, 25–31], when it is nanosized on an oxide support. The source of this activity is still unclear. It is suggested to be associated with a quantum-size effect [7], support-induced strain [19], charge transfer from the small gold particles to adsorbed oxygen [32] and the role of low-coordinated gold atoms [19, 21–24]. It has also been suggested that the catalytic activity could perhaps be influenced by a relativistic effect on the 6s orbital of the heavier elements, especially Pt and Au [32a]. The major drawback to gold is its low melting point that can lead to sintering of gold nanoparticles [33–35] and then the activity may not be sufficient for an application at elevated temperatures. For catalytic reactions that take place on gold even at room temperature – such as CO oxidation – sintering of nanoparticulate gold has not been reported to occur.

Recently, we reported that CH_4 oxidation on TiO_2 supported gold nanoparticles proceeds at low temperature with a strong tendency to form CO_2 [36]. Partial oxidation of CH_4 to CO and H_2 has been studied on various other supported noble metal catalysts by Baiker et al., who reported rates and selectivity between 300°C and 500°C [37]. For a Pt/Al_2O_3 catalyst it was recently reported that oxygen-rich surfaces seem to suppress the dissociative adsorption of CH_4, resulting in low CH_4 oxidation activity in excess oxygen [38]. At high temperatures (600°C – 800°C), it has been shown through isotope labeling studies on CH_4 reforming reactions over supported platinum clusters, that CO_2 activation steps are

much faster than the kinetically relevant steps for CH_4 chemical conversion to synthesis gas [39]. The authors conclude in that study, that CO_2 activation steps must be quasi-equilibrated and kinetically irrelevant. Recent studies suggest that there is a condition dependent mechanism for the reforming reaction of CH_4 with CO formation being dominant at lower temperatures and CH_4 activation taking over at higher temperature [40].

In the present contribution, we focus on low-temperature CH_4 oxidation on various metal-oxide supported gold catalysts. The main objective in this experimental work is to study the contribution of the metal-oxide support to the catalytic reaction for different support materials. We present our findings based on steady-state activity measurements and TEM analysis. Another issue was to check whether by changing the support one could avoid the final oxidation step of CO to CO_2 at low temperature.

Experimental section

Experimental equipment

Steady-state activity measurements of various metal-oxide supported gold catalysts were performed in mini-reactors. These mini-reactors are basically quartz glass tubes with a reactor volume of approximately 250 mm^3. They were heated using a hotplate. The temperature was measured with a K-type thermocouple and controlled using a PID-controller (Eurotherm). The reactants, CH_4 (5.5 purity) and O_2 (3.5 purity), were supplied and controlled using mass flow controllers (Bronkhorst). The total gas flow was kept constant for all measurements at 0.50 ml min^{-1}. The reaction products were analyzed using an Agilent gas chromatograph (3000A microGC). The GC has combined columns of 10 m molecular sieve and 3 m PLOT U with 1.0 µl back-flushing, which allows simultaneous analysis of CH_4, O_2, N_2, CO, CO_2, H_2, H_2O, C_2H_6, HCHO and CH_3OH by a thermal conductivity detector (TCD). With argon as the carrier gas, the GC is 15 times more sensitive to H_2 than to CO, and a C_2H_6 concentration below 0.01% could still be detected. To avoid condensation of water, formed by the catalytic reactions, the tubing between the mini-reactor and the GC was kept at a temperature of 100°C, whereas the capillary of the GC itself was kept at 90°C.

Method

Three different 2.0 nm gold catalysts (AURO*lite*™) were supplied by Project AuTEK [41]:

(A) Au/TiO_2 (1.02 wt% Au),
(B) Au/ZnO (0.978 wt% Au),
(C) Au/Al_2O_3 (0.84 wt% Au).

These powder catalysts had been prepared by carefully developed methods involving gold precipitation from solution [41]. To ensure reproducibility, each catalyst was first activated by a pre-treatment of 10 hours at 100°C and continuous gas flow of CH_4 and O_2 in the ratio of 1:2 as well as a temperature ramp from 30°C to 250°C in steps of 10°C h^{-1}, before the following sequence of CH_4:O_2 ratios was used: 1:2, 1:1, 2:1. The reaction according to the first step of the sequence was re-measured to confirm that the catalyst did not change during the reactions. To verify that the applied gases did not alter the catalysts, the described schemes were run once more in inverse order using a fresh catalyst. For steady-state activity measurements, the temperature was ramped from 30°C to 250°C in steps of 10°C h^{-1}.

Self heating of the catalyst during an exothermic reaction is difficult to avoid, but it can be minimized by operating the catalyst in the lower range of its kinetically controlled regime. The greatest amount of heat liberated during the reaction was 16.9 mW when CH_4 and O_2 were applied in the stoichiometric ratio to form CO_2 and H_2O at 250°C.

Particle analysis

To confirm the particle size and the purity of the catalyst as stated by the supplier, we used both transmission electron microscopy (TEM) and X-ray fluorescence (XRF). For the latter technique, we used a Minipal 4 X-ray spectrometer (PANalytical). The size distribution and shape of the gold particles were probed using a Tecnai 20T TEM operating at 200 kV. Specimens of the catalyst were taken before and after the temperature-programmed activity measurements, and prepared on a carbon TEM grid. Detection of particles in a TEM image is usually performed by transforming the grayscale image into a binary image by *thresholding* the *whole* picture at once using a 'global threshold' value. This approach works well if all of the particles are dark enough with respect to the background intensity in the image, but often fails because of local changes in the contrast of the TEM image. Here, instead, an algorithm based on local thresholding was applied to improve the detection of the particles.

Results

The purity of the catalysts used was checked using XRF. Catalyst B contained traces of Fe and Ni, in catalyst C were found traces of Fe and Cu, whereas impurities in catalyst A must have been below the detection limit of the system used. To study the influence of the pre-treatment and the catalytic reactions on the catalysts, TEM images were taken of specimens of the catalysts as supplied, after pre-treatment and after steady-state activity measurements. The average particle size of the catalysts, 2.0 nm, as stated by the supplier, could be confirmed for A and B, whereas C was found to be larger: 2.8±1.3 nm. Since Al_2O_3 is not a reducible metal oxide like TiO_2 or ZnO, to which oxygen vacancies usually are referred to be anchoring points for deposited nanoparticles, an enhanced sintering effect cannot be excluded. Probably, the gold particles were already sintered during storage.

Figure 1

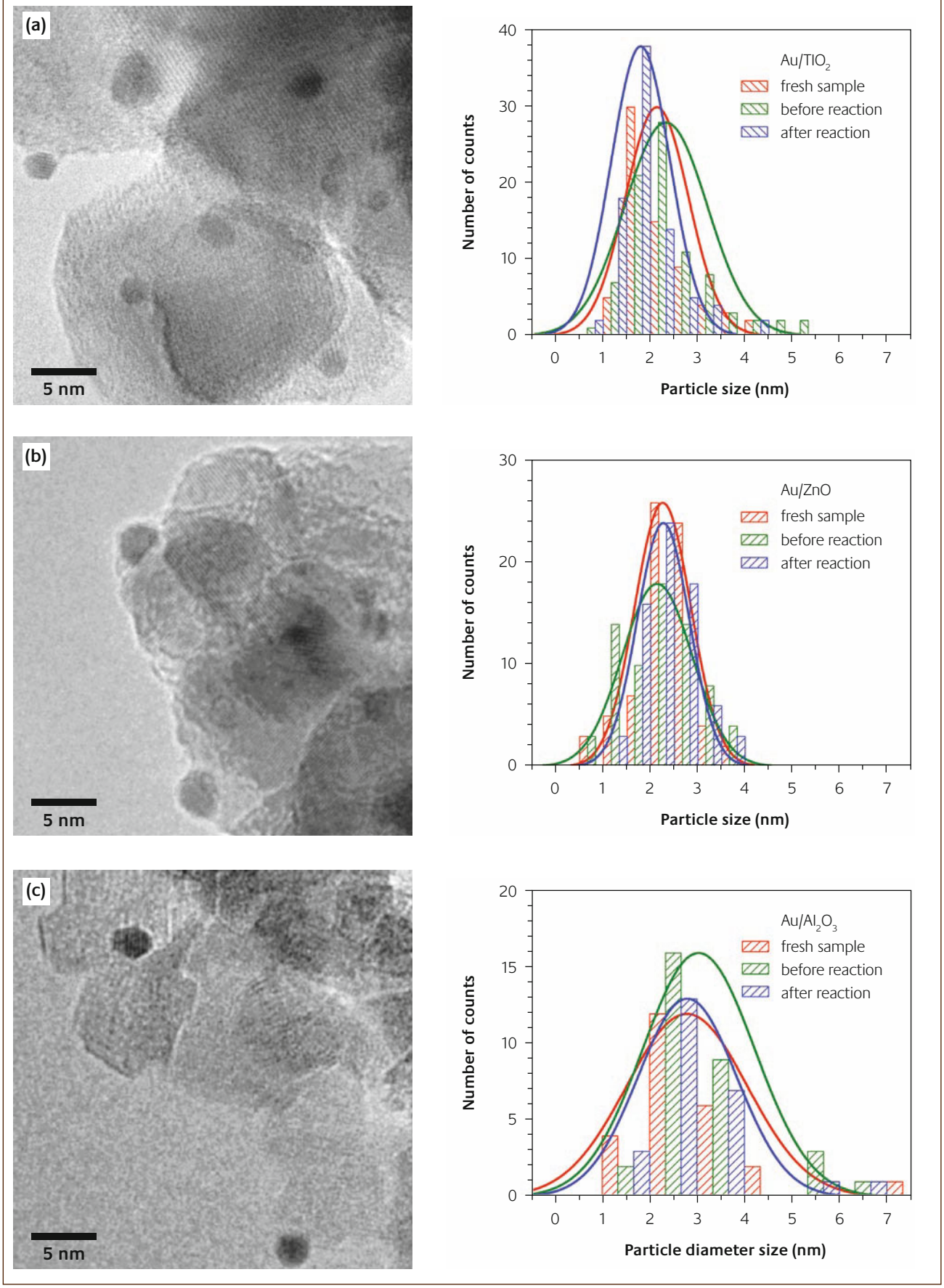

TEM image of the catalysts A, B and C after methane oxidation reactions together with the statistical analysis of the average particle size from all states of the catalysts – fresh (as supplied), after pre-treatment and after reactions – in the figures (a), (b) and (c), respectively

TEM analysis on changes in particle size

Figure 1(a) shows a typical TEM image of Catalyst A after reaction. Remarkably, the particle size did not change drastically, either during the pre-treatment – *cf*. the red and the green distribution curves, or due to methane oxidation – *cf*. the green and the blue distribution curves in the graph below. After the reaction, the gold particles' size was determined to be 1.8±0.6 nm based on a TEM analysis of 81 particles. This behavior is in strong contrast to measurements after CO oxidation over a fresh catalyst of the same batch, that have been conducted at much lower temperatures than applied in this study [42], where substantial sintering was found. Our recent findings for CO oxidation on the same material as used for Catalyst A might have been affected by the use of different oxidation agents: O_2 and N_2O.

The TEM image in Figure 1(b) shows gold particles observed after reaction on catalyst B. The average particle size was determined to be 2.3±0.6 nm. Also this catalyst was very stable, since the particle size did not change significantly.

Catalyst C contained right from the beginning bigger gold particles. The measurement of particle sizes from TEM images was difficult due to the high contrast of the Al_2O_3 crystals supporting the nanoparticles, and curves must be interpreted with caution. However, the size distribution indicates average particle sizes greater than that of the other two catalysts. After the reaction, the average particle size was still 2.8±1.0 nm.

Steady-state activity measurements

From the Arrhenius plots in Figure 2, the apparent activation energies for CH_4 oxidation on the three different catalysts evaluated were determined to be approximately the same for the feed gas ratio of $CH_4 : O_2 = 1:2$. The values are summarized in Table 1. The specific CH_4 oxidation rate indicates clearly that catalyst A was the most active one. For this catalyst the conversion of CH_4 to CO_2 according to equation (4) was greatest with 29% at 250°C, as is shown in Figure 3. Also, in this figure it may clearly be seen that the CH_4 conversion begins already at 130°C when using Catalyst A. For Catalysts B and C, we found the onset of conversion to be at around 150°C. Since neither CO nor other organic chemicals were detected for this feed gas ratio, which according to Equations (1) – (3) would be an indication that partial CH_4 oxidation occurs, the yield of CO_2 is directly given by the consumption of CH_4. The onset of CH_4 oxidation was found to be 130°C for Catalyst A. On the other catalysts, CH_4 oxidation did not take place at temperatures below 150°C.

Besides the results shown here for an applied feed gas ratio of $CH_4 : O_2 = 1:2$, it is worth mentioning that traces of C_2H_6 could only be detected on Catalyst A and when the feed gas of reactants was applied in a ratio of $CH_4 : O_2 = 2:1$. Considering the reaction represented by Equation 5 the greatest yield of C_2H_6 would be expected for $CH_4 : O_2 = 4:1$.

$$2\ CH_4 + {}^1/_2\ O_2 \rightarrow C_2H_6 + H_2O \qquad \Delta H^0 = -176.9\ kJ\ mol^{-1} \qquad (5)$$

This could be confirmed in a separate measurement. The yield of C_2H_6 increased to 0.03% at 250°C, whereas the yield of CO_2 dropped down to 13%, when a ratio of $CH_4 : O_2 = 4:1$ was applied. No other products could be detected.

Figure 2

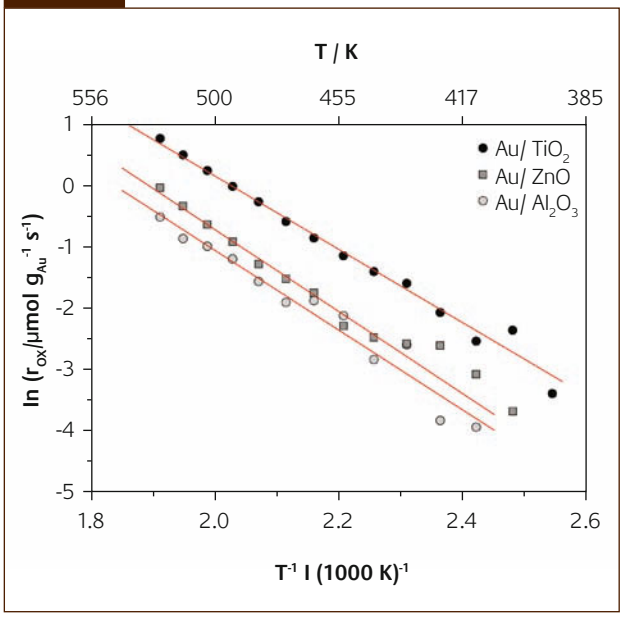

Arrhenius plots of the specific CH_4 oxidation rates: Catalyst A (●), Catalyst B (■), Catalyst C (o). The apparent activation energies are summarized in Table 1

Figure 3

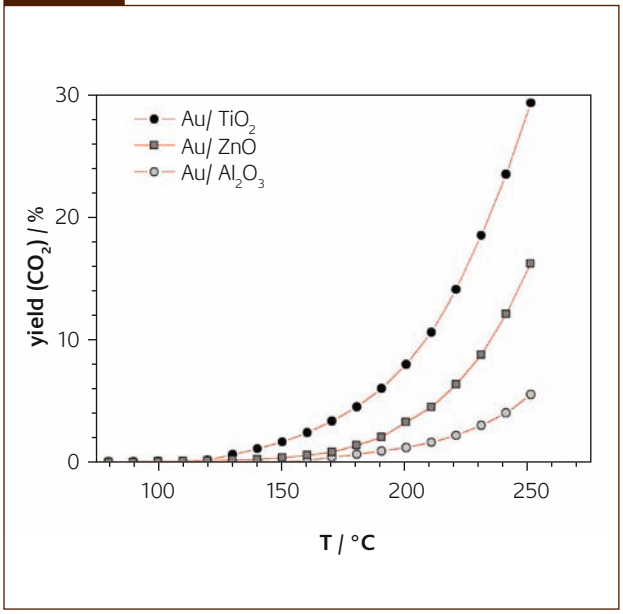

CH_4 conversion begins at 130°C when using Catalyst A (●), whereas for the Catalysts B (■) and C (o), the onset of conversion is around 150°C.

Discussion

Table 1 shows that the influence from the support material plays a minor role compared with the reduction of the overall reaction barrier: the apparent activation energies did not vary significantly. Concerning the specific rate for CH_4 oxidation, Catalyst A provided the highest turnover numbers of all the catalysts tested. This is probably also related to the fact that Catalyst A had the smallest gold nanoparticles. If we keep in mind that all the catalysts used were prepared by the same preparation method, it can be concluded from these results that TiO_2 is a good support for catalytically active gold. Compared to CO oxidation, we should note that the specific oxidation rate for CH_4 oxidation is, however, more than 150,000 times less than for CO oxidation on a catalyst of the same batch, already observed at a temperature of 80°C [42].

In addition to the activity, we addressed the issue of stability by investigating changes in particle size using TEM. From our observations, nanosized gold seems to be inhibited from sintering during CH_4 oxidation. For a catalyst of the same batch as Catalyst A, Ref. [42] presents a thorough study of CO oxidation using O_2 and N_2O as oxidation agent. These reactions proceed at temperatures below 80°C. However, it is also shown that even at such low temperatures sintering of gold nanoparticles occurs when N_2O is used. On the other hand, a similar non-sintering phenomenon was reported for alumina supported gold catalysts when 3*d*-metal oxides are added [43]. But it also has to be borne in mind that the catalysts in that study were first calcined at 400°C in O_2 and this led to sintering. Thus the particle size and the – still unidentified – active sites available, are not comparable with those of Catalyst C in our study. The results presented in this contribution are based on temperature programmed reaction experiments that had kept the catalyst at or above 200°C for 30 hours. To clarify whether the observed non-sintering phenomena is associated with CH_4 or OH present during the reaction, further research needs to be done.

Concerning the measured C_2H_6, three points are worth mentioning:

(a) The measurements with a CH_4: O_2 ration of 4:1 show an enhancement in the C_2H_6 yield compared to those where the ratio is 2:1. Therefore, we can firstly conclude that C_2H_6 is a by-product of the reaction studied, and secondly that since the yield was only 0.03% in C_2H_6, gold has a high selectivity for CO_2. (b) Comparing equations (2) and (5), C_2H_6 formation is thermodynamically less likely than HCHO formation. The reason why C_2H_6 is formed instead needs further investigations. (c) The presence of C_2H_6 implies that there must be a pathway to dissociate CH_4 such that two methyls may recombine subsequently.

Another interesting issue is the strong tendency to form CO_2 irrespective of the support used, as it can be seen in the activity measurements presented. During CH_4 oxidation, we observed H_2O and CO_2 formed in a stoichiometric ratio as expected from Equation (4). From this result, we conclude that complete combustion of CH_4 takes place over all supports. Recent studies [36, 42] show that the lower overall barrier for CO oxidation (36 kJ mol^{-1} vs. 50 kJ mol^{-1} for CH_4 oxidation (*cf.* Table 1)) indicates that under these reaction conditions the post-oxidation of CO proceeds much faster than the oxidation of an adsorbed CH_4 species. Thus, for the overall reaction of CH_4 oxidation the elementary steps following the formation for CO_2 would be quasi-equilibrated. It is suggested that in a similar fashion the elementary steps for H_2 may well be quasi-equillibrated on this catalyst. Support for this viewpoint is that the overall barrier for H_2 oxidation is much lower as well (38 kJ mol^{-1}) [42]. Furthermore, atomic H (liberated from CH_4) might perhaps already form H_2O at an even lower activation barrier. This means that CH_4 oxidation is the rate-limiting step of the overall reaction for each of the support materials tested.

Conclusions

In this contribution, we have described investigations on various metal-oxide supported gold catalysts in terms of CH_4 oxidation under mild conditions (1 bar, 30°C – 250°C). Steady-state activity measurements show that CO_2 was formed with a high selectivity by complete combustion of CH_4 irrespective of the support used. Although nanoparticular gold is known to sinter even at low temperature during other reactions, we did not find any indication of sintering from our TEM analysis. Further research needs to be done to clarify what causes the stability of gold under these conditions. Finally, we conclude that TiO_2 is the best support of those tested.

Table 1

Comparison of activation energies, reaction rates and yield of CO_2 at 250°C as well as the particle size determined using TEM

	Total Au loading / mg	d_{Au}/nm	E_a/kJ mol^{-1}	ln(r_{ox} / µmol g_{Au}^{-1} s^{-1})	yield (CO_2) /%
Catalyst A	9.90	1.8 ± 0.6	50 ± 1.1	0.77	29.4
Catalyst B	11.43	2.3 ± 0.6	56 ± 1.7	-0.04	16.3
Catalyst C	6.34	2.8 ± 1.0	53 ± 3.4	-0.52	5.6

Acknowledgements

G. Walther gratefully acknowledges financial support from NABIIT and the support of gold catalysts from Project AuTEK. We also thank D.T. Thompson for stimulating discussions.

About the authors

Guido Walther received his diploma in physics from the Heinrich-Heine University in Düsseldorf, Germany, in 2004 and his PhD from the Technical University of Denmark (DTU) in 2008. His research interests include catalysis by precious metals and hydrocarbon chemistry. He is currently employed as Post-doc at the Leibniz Institute for Catalysis in Rostock, Germany.

Lionel Cervera-Gontard studied physics at the University of Seville (Spain) and did his PhD in England on the application and development of TEM techniques for the study of heterogeneous catalyst nanoparticles. He now works as a Post-doc in the Center for Electron Nanoscopy (CEN) at DTU.

Ulrich Joachim Quaade received his Cand. Scient. in physics and mathematics in 1993 and his PhD in 1995 from Odense University, Denmark. From 1995 to 2001 he was Associate Research Professor at the Microelectronic Centre (MIC) at DTU. From 2001 he was Associate Professor at the Physics Department (DTU) until 2008, when he moved on to Amminex, a spin-off company from DTU.

Sebastian Horch received his Physics Diploma in 1991 and his Dr. rer. nat. in 1994 from Bonn University, Germany. After a Feodor Lynen Research Fellowship at Arizona State University, he moved to the Center for Atomic-scale Materials Physics (CAMP) at Aarhus University, Denmark as Assistant Research Professor in 1996. Since 1999 he is Associate Professor at the Physics Department (DTU). In the Center for Individual Nanoparticle Functionality (CINF), he mainly applies Scanning Probe Microscopy to study catalysts on the nanoscale.

References

1 V.S. Arutyunov, V.M. Rudakov, V.I. Savchenko, E.V. Sheverdenkin, O.G. Sheverdenkin and A.Yu. Zheltyakov, *Theo. Found. Chem. Eng.*, 2002, **36**, 472
2 C.-J. Liu, T. Hammer and R. Mallinson, *Catal. Today*, 2004, **98**, VII
3 M.O. Adebajo, *Green Chem.*, 2007, **9**, 526
4 N.D. Parkyns, C.I. Warburton and J.D. Wilson, *Catal. Today*, 1993, **18**, 385
5 G.A. Olah and Á. Molnár, *Hydrocarbon Chemistry*, Wiley-Interscience, 2003
6 M. Haruta, *Catal. Today*, 1997, **36**, 153
7 M. Valden, X. Lai and D.W. Goodman, *Science*, 1998, **281**, 1647
8 G.C. Bond and D.T. Thompson, *Catal. Rev. – Sci. Eng.*, 1999, **41**, 319
9 M. Haruta, *Cat. Tech.*, 2002, **6**, 102
10 A.C. Gluhoi, M.A.P. Dekkers and B.E. Nieuwenhuys, *J. Catal.*, 2003, **219**, 197
11 B. Schuhmacher, V. Plzak, M. Kinne and R.J. Behm, *Catal. Lett.*, 2003, **89**, 109
12 M. Chen and D.W. Goodman, *Science*, 2004, **306**, 252
13 T.V.W. Janssens, A. Carlsson, A. Puig-Molina and B.S. Clausen, *J. Catal.*, 2006, **240**, 108
14 H.-J. Freund, *Catal. Today*, 2006, **117**, 6
15 G.C. Bond, C. Louis and D.T. Thompson, *Catalysis by Gold*, Imperial College Press, 1. Edition, London, 2006
16 D.T. Thompson, *Topic. Catal.*, 2006, **38**, 231
17 C. Xu, J. Su, X. Xu, P. Liu, H. Zhao, F. Tian and Y. Ding, *J. Am. Chem. Soc.*, 2007, **129**, 42
18 B. Hammer, J.K. Nørskov, *Surf. Sci.*, 1995, **343**, 211
19 M. Mavrikakis, P. Stotze, J.K. Nørskov, *Catal. Lett.*, 2000, **64**, 101
20 Z. Liu, P. Hu and A. Alavi, *J. Am. Chem. Soc.*, 2002, **124**, 14770
21 N. Lopez and J.K. Nørskov, *J. Am. Chem. Soc.*, 2002, **124**, 11262
22 N. Lopez, T.V.W. Janssens, B.S. Clausen, Y. Xu, M. Mavrikakis, T. Bligaard and J.K. Nørskov, *J. Catal.*, 2004, **223**, 232
23 T.V.W. Janssens, B.S. Clausen, B. Hvolbæk, H. Falsig, C.H. Christensen, T. Bligaard, and J.K. Nørskov, *Topic. Catal.*, 2007, **44**, 15
24 B. Hvolbæk, T.V.W. Janssens, B.S. Clausen, H. Falsig, C.H. Christensen, and J.K. Nørskov, *NanoToday*, 2007, **2**, 14
25 R.D. Waters, J.J. Weimer and J.E. Smith, *Catal. Lett.*, 1994, **30**, 181
26 S. Ivanova, C. Petit, V. Pitchon, *Catal. Today*, 2006, **113**, 182
27 S. Ivanova, C. Petit, V. Pitchon, *Gold Bulletin*, 2006, **39**, 3
28 B.E. Solsona, T. Garcia, C. Jones, S.H. Taylor, A.F. Carley and G.J. Hutchings, *Appl. Catal. A*, 2006, **312**, 67
29 A.S.K. Hashmi and G.J. Hutchings, *Angew. Chem. Int. Ed.*, 2006, **45**, 7896
30 C.H. Christensen, B. Jørgensen, J. Rass-Hansen, K. Egeblad, R. Madsen, S.K. Klitgaard, S.M. Hansen, M.R. Hansen, H.C. Andersen and A. Riisager, *Angew. Chem. Int. Ed.*, 2006, **45**, 4648
31 M.C. Daniel and D. Astruc, *Chem. Rev.*, 2004, **104**, 293
32 J.A. v. Bokhoven, C. Louis, J.T. Miller, M. Trommp, O.V. Safonova and P. Glatzel, *Angew. Chem.*, 2006, **118**, 4767
32a G.C. Bond, *Catal.Today*, 2002, **72**, 5
33 P. Buffat and J.P. Borel, *Phys. Rev. A*, 1976, **13**, 2287
34 E. Charls, H. Sykes, F.J. Williams, M.S. Tikhov and R.M. Lambert, *J. Phys. Chem. B*, 2002, **106**, 5390
35 P.M. Ajayan and D.L. Marks, *Phys. Rev. Lett.*, 1988, **60**, 585

36 G. Walther, G. Jones, S. Jensen, U.J. Quaade, S. Horch, *Catal. Today*, 2009, **142**, 24
37 S. Hannemann, J.-D. Grunwaldt, P. Lienemann, D. Günther, F. Krumeich, S.E. Pratsinis and A. Baiker, *Appl. Catal. A* , 2007, **316**, 226
38 E. Becker, P.-A. Carlsson, H. Grönbeck and M. Skoglundh, *J. Catal*., 2007, **252**, 11
39 J. Wei and E. Iglesia, *J. Phys. Chem. B*, 2004, **108**, 4094
40 M.P. Andersson, F. Abild-Pedersen, I.N. Remediakis, T. Bligaard, G. Jones, J. Engbæk, O. Lytken, S. Horch, J.H. Nielsen, J. Sehested, J.R. Rostrup-Nielsen, J.K. Nørskov and I. Chorkendorff, *J. Catal*., 2008, **255**, 6
41 http://www.mintek.co.za.
42 G. Walther, D.J. Mowbray, T. Jiang, G. Jones, S. Jensen, U.J. Quaade, S. Horch, *J. Catal*., 2008, **260**, 86
43 R.J.H. Griesel and B.E. Nieuwenhuys, *Catal. Today*, 2001, **64**, 69